Hindawi
Advances in High Energy Physics
Volume 2024, Article ID 5195790, 11 pages
https://doi.org/10.1155/2024/5195790

Research Article

Solving Schrödinger Wave Equation for the Charmonium Spectrum Using Artificial Neural Networks

Tariq Mahmood ,[1] Jumanah Ahmed Darwish,[2] Talab Hussain,[1] Maqsood Ahmed,[1] and Rehan Ahmad Khan Sherwani[3]

[1]*Centre for High Energy Physics, University of the Punjab, Lahore, Pakistan*
[2]*Department of Mathematics and Statistics, College of Science, University of Jeddah, Jeddah, Saudi Arabia*
[3]*College of Statistical Sciences, University of the Punjab, Lahore, Pakistan*

Correspondence should be addressed to Tariq Mahmood; tariqmahmood.chep@pu.edu.pk

Received 21 August 2023; Revised 28 December 2023; Accepted 31 January 2024; Published 3 April 2024

Academic Editor: John Strologas

In this study, we solved the Schrödinger wave equation by using effective potential in an artificial neural network (ANN) for the mass spectrum of different charmonium states, including η_c, ψ_2, χ_2, and χ_4. The ANN approach provides an efficient, more general, and continuous solution-approximating strategy, thus eliminating the possibility of skipping any region of interest in mass spectroscopy. The close consistency of ANN results with the already-reported results from numerical and theoretical approaches and experimental ones shows the reliability and accuracy of the ANN approach.

1. Introduction

Researchers from the area of high-energy physics primarily investigate the particles' interactions (gravitational, strong, electromagnetic, and weak) at the fundamental level of the universe through experiments utilizing accelerator and detector technology and an elegant theory known as the Standard Model of Particle Physics [1, 2]. The Standard Model was developed to effectively explain physical processes concerning fundamental interactions (excluding gravity) and becomes the well-tested theory of physics by precisely predicting outcomes of different phenomena [1].

In quantum chromodynamics (QCD), because of color charge, quarks interact through strong forces, whereas spin-one particles, such as chargeless photons and gluons with bicolor charge (conserved in strong interaction), are the exchange particles of quantum electrodynamics (QED) and QCD, respectively. Coupling constants $\alpha = e^2/4\pi\epsilon_0\hbar c$ and $\alpha_s = g^2/4\pi$ are dimensionless quantities and considered to be the interaction strengths in QED and QCD, respectively [3], where e is the electric charge, ϵ_0 is the permittivity of free space, $\hbar$ is the reduced plank constant, c is the speed of light, and g is the color charge.

With the increase in Q^2 (momentum transfer squared), QED α increases, while QCD α_s decreases. In quantum electrodynamics, because of the minimal values of the coupling constant α, we can perform calculations perturbatively [4]. Hadron's proper solution of the mass spectrum is not achievable because in QCD, perturbative calculations are only valid at high energies (small α_s) and not valid at low energies (large α_s). For this, different models exist to investigate the low-energy process of QCD [5].

Numerov's matrix method [6], shooting method [7], and Crank-Nicolson's approach [8] are the numerical methods to solve the Schrödinger wave equation. Artificial neural networks, which were introduced in the field of high-energy physics in 1988 [9], can handle the increase in the complexity of data in physics processes, as reviewed in [10]. In solving ordinary and partial differential equations, ANNs have the following advantages over the existing numerical methods [11].

(i) ANNs, being universal approximators, can solve differential equations

(ii) The dimensionality and sampling point of the problems do not affect the trial solution or complexity of ANNs

(iii) For all domain points, ANN gives us continuous solutions as compared to the different numerical techniques

2. Literature Review

Artificial neural networks are being used to solve different problems relevant to the optimization of high-energy physics processes [12–17]. In theoretical HEP, artificial neural networks are being used to calculate the mass spectra of particles by solving the Schrödinger wave equation [16–20], while in experimental high-energy physics, artificial neural networks are being used in event classification [21, 22], object reconstruction [23, 24], triggering [25, 26], and track fitting [27, 28]. Apart from these, artificial neural networks are also being used to solve quantum many-body problems [29] through ordinary and partial differential equations in different domains [30–32]. Recent advancements in machine learning and high-energy physics have also highlighted the use of quantum neural networks [33–36].

In 1997, Lagaris et al. used ANNs to solve the Schrödinger wave equation and Dirac equation for the ground state energy of muonic atoms using Morse Hamiltonian by considering the finite protonic charge distribution as well as the vacuum polarization effective potential. They also compared the results with the finite element method and showed that ANN is far more economical and efficient [37].

In 1998, Lagaris et al. described the advantages of neural networks over numerical techniques. They used neural networks to solve those ordinary and partial differential equations that require function approximation for the solution written in differentiable and closed analytical form. Their proposed model consisted of the sum of two terms: the initial/boundary conditions term to satisfy with no adjustable parameters. The second term contains the ANN term, which is to be trained to satisfy the differential equation by adjusting the parameters of the neural network (weights and biases) to minimize the error function. Through this model of ANN, they solved many examples of ordinary and partial differential equations for different problems. They compared their results with the finite element method and concluded that ANN has excellent generalization performance over the numerical technique [30].

In 2001, Sugawara solved the Schrodinger wave equation for a one-dimensional harmonic oscillator using the Morse potential [38], which showed how powerful artificial neural networks and genetic algorithms can be. In 2004, Damazio and de Seixas used neural networks to identify particles using the topological properties of calorimeters [39].

In 2008, Teodorescu argued that during the last decade, ANNs were commonly used in experiments [40], such as CDF [41], BABAR [42], and DZero [43]. In 2006, Miranker derived a complete wave formalism for information transmission in the neural network by using a novel Lagrange form of the canonical neural network equation. In this study, the author also derived the neural network-based Schrödinger wave equation for the time-dependent evolution of the quantum mechanical system [44]. In 2013, Therhaag highlighted the use of neural networks in the field of high-energy physics to solve the classification task of separating exciting data (signal) from unwanted noise (background) [45].

In 2013, Radi and Hindawi also reported the use of machine learning techniques such as neural networks (ANN), genetic algorithms (GA), genetic programming (GP), and gene expression programming to understand the interactions of the fundamental particles in the field of high-energy physics [46]. In 2014, Sadowski et al. used a data set of 82 million simulated collision events for the training of an artificial neural network to detect the decay of Higgs bosons to tau leptons. He suggested that neural networks can automatically discover high-level features from the data [47]. In 2018, Mutuk also used the trial function method based on neural networks to solve the Blasius differential equation for fluid mechanics and compared the results with the existing numerical techniques [16]. Baldi et al. [14] used a parameterized neural network for the analysis and prediction of new particles in the field of high-energy physics.

In 2020, Hermann et al. solved many electrons in the Schrödinger wave equation using a deep neural network. They accurately represented the ground state energies of He, H2, Be, B, LiH, and a chain of 10 hydrogen atoms [48]. In 2018, Mutuk used a neural network to figure out the energy levels of a quartic anharmonic oscillator in one dimension. He then showed that the proposed method (ANN) was accurate by comparing the results to other numerical methods [49].

In 2019, Mutuk solved the Schrödinger wave equation for different cases of Cornell potential and compared the calculated charmonium, bottomonium, and bottom-charmed spin-averaged spectra with the already existing theoretical and experimental results [17]. In 2019, Mutuk also used a neural network to solve the 5-body Schrödinger equation in the framework of the nonrelativistic quark model with four different types of potential and predicted the parities of the states that were not determined in the observation of hidden-charm pentaquark states announced in the LHCb experiment [20].

In 2019, Mutuk used a neural network to investigate the mass spectra of the strange X (5568) state and its possible charmed partner Xc. He then compared his predictions with both theoretical and experimental data [19]. In 2020, Sharma, as a prospect, also highlighted the supremacy of quantum machine learning in high-energy physics [50]. In 2020, Manzhos provided a comprehensive review of the use of neural networks for the solution of the vibrational Schrödinger equation, the electronic Schrödinger equation, and the related problems of density functional theory [51]. Lema and Choromanska [52] trained an artificial neural network in an unsupervised learning framework by finding the best expectation value for particles in a box with and without

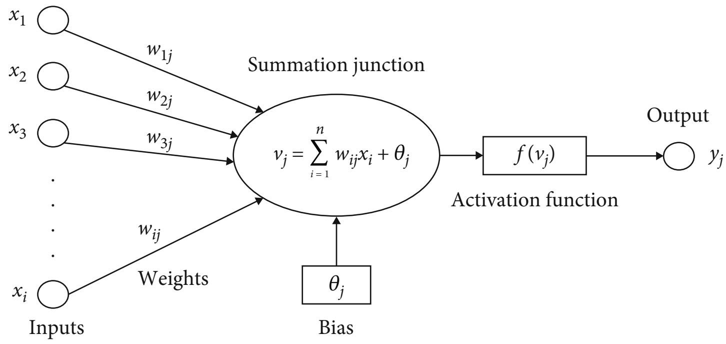

Figure 1: Working of artificial neuron.

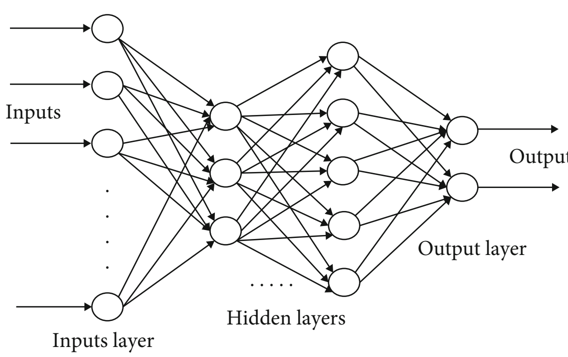

Figure 2: Multilayer artificial neural network.

perturbation. This led to a very accurate prediction of ground state energies and wave functions [52].

In this work, the Schrödinger wave equation is solved for QCD's complete potential for the charmonium system using an artificial neural network. The computed results are compared with the existing theoretical and experimental results to verify the predictability, accuracy, and precision of neural results. In Section 3, we provide the detailed implementation of an artificial neural network for a charmonium system. In Section 4, we have discussed our numerical results for the eigenvalues for the QCD complete potential of the charmonium system. In Section 5, we have concluded our findings in view of future perspectives.

3. Methodology

A neural network is a massively parallel, distributed processor made up of simple processing units (artificial neurons). It has many advantages over the semianalytic and numerical methods for solving the ordinary and partial differential equations discussed in the previous section. In the human brain, an information processing unit is a neuron that is used to construct the neural network. Figure 1 illustrates the perceptron with multiple inputs summed up to z and one output, which is calculated with the help of the nonlinear function $\sigma(z)$, where $\sigma(z)$ can be any function for which it is possible to derive all the derivatives of $\sigma(z)$ in terms of itself.

Feed-forward neural networks, due to their structural flexibility, good symbolic capabilities, and availability of many training algorithms, are the most famous architecture. A feed-forward neural network shown in Figure 2 consists of input, hidden, and output layers of neurons that are fully connected.

The input-output properties can be written as follows:

$$\begin{aligned} O_i &= \sigma(n_i), \\ O_j &= \sigma(n_j), \\ O_k &= \sigma(n_k), \end{aligned} \tag{1}$$

where i, j, and k are the indices for input, hidden, and output layers, respectively, and n is the number of neurons. Input to the neural network is given as follows:

$$\begin{aligned} n_i &= (\text{input signal to the NN}), \\ n_j &= \sum_{i=1}^{N_i} w_{ij} O_i + \theta_j, \\ n_k &= \sum_{j=1}^{N_j} w_{jk} O_j + \theta_k, \end{aligned} \tag{2}$$

where w_{ij} is the weight signal connecting the ith neuron of the input layer to the jth neuron of the hidden layer, w_{jk} is the weight signal connecting the jth neuron of the hidden layer to the kth neuron of the output layer, and θ_j and θ_k are the threshold-biased parameters for the hidden and output layers. The overall output can be calculated as follows:

$$O_k = \sigma\left(\sum_{j=1}^{N_j} w_{jk}\sigma\left(\sum_{i=1}^{N_i} w_{ij} n_i + \theta_j\right) + \theta_k\right). \tag{3}$$

Table 1: Comparison of our calculated masses of ground and radially excited states of charmonium mesons using an artificial neural network with other predicted theoretical and experimental results.

n	Meson	L	S	J	Our calculated mass using an artificial neural network (GeV)	Theoretical mass [53] using the shooting method (GeV)	Theoretical mass [54] with NR potential model (GeV)	Exp. mass (GeV) [55]
1S	$\eta_c(1^1S_0)$	0	0	0	2.98101	2.9816	2.982	2.9810 ± 0.0011
	$J/\psi(1^3S_1)$	0	1	1	3.0953	3.08999	3.090	3.096916 ± 0.0001
2S	$\eta_c(2^1S_0)$	0	0	0	3.63890	3.6303	3.630	3.6389 ± 0.0013
	$J/\psi(2^3S_1)$	0	1	1	3.68611	3.6718	3.672	$3.6861^{+0.000012}_{-0.000014}$
3S	$\eta_c(3^1S_0)$	0	0	0	4.0430	4.0432	4.043	—
	$J/\psi(3^3S_1)$	0	1	1	4.04000	4.0716	4.072	4.040 ± 10 [54]
4S	$\eta_c(4^1S_0)$	0	0	0	4.38400	4.3837	4.384	—
	$J/\psi(4^3S_1)$	0	1	1	4.41500	4.4061	4.406	4.415 ± 6 [54]
1P	$h_c(1^1P_1)$	1	0	1	3.5255	3.5156	3.516	3.52541 ± 0.00016
	$\chi_0(1^3P_0)$	1	1	0	3.4149	3.4233	3.424	3.41475 ± 0.00031
	$\chi_1(1^3P_1)$	1	1	1	3.51070	3.5005	3.505	3.51066 ± 0.00007
	$\chi_2(1^3P_2)$	1	1	2	3.5583	3.5490	3.556	3.55620 ± 0.00009
2P	$h_c(2^1P_1)$	1	0	1	3.9344	3.9336	3.934	—
	$\chi_0(2^3P_0)$	1	1	0	3.8519	3.8715	3.852	—
	$\chi_1(2^3P_1)$	1	1	1	3.9256	3.9203	3.925	—
	$\chi_2(2^3P_2)$	1	1	2	3.9272	3.9648	3.972	3.9272 ± 0.0026
3P	$h_c(3^1P_1)$	1	0	1	4.279	4.2793	4.279	—
	$\chi_0(3^3P_0)$	1	1	0	4.202	4.2295	4.202	—
	$\chi_1(3^3P_1)$	1	1	1	4.26695	4.2663	4.271	—
	$\chi_2(3^3P_2)$	1	1	2	4.3171	4.3093	4.317	—
4P	$h_c(1^1P_1)$	1	0	1	4.58500	4.5851	—	—
	$\chi_0(4^3P_0)$	1	1	0	4.5425	4.5424	—	—
	$\chi_1(4^3P_1)$	1	1	1	4.57201	4.5720	—	—
	$\chi_2(4^3P_2)$	1	1	2	4.6141	4.6141	—	—
1D	$\eta_{c2}(1^1D_2)$	2	0	2	3.799001	3.7994	3.799	—
	$\psi(1^3D_1)$	2	1	1	3.7699	3.7805	3.785	3.7699 ± 0.0025 [54]
	$\psi_2(1^3D_2)$	2	1	2	3.8000	3.8002	3.800	—
	$\psi_3(1^3D_3)$	2	1	3	3.8060	3.8053	3.806	—
2D	$\eta_{c2}(2^1D_2)$	2	0	2	4.1580	4.1576	4.158	—
	$\psi(2^3D_1)$	2	1	1	4.1590	4.1363	4.142	4.159 ± 0.020 [54]
	$\psi_2(2^3D_2)$	2	1	2	4.158	4.1580	4.158	—
	$\psi_3(2^3D_3)$	2	1	3	4.167	4.1655	4.167	—
3D	$\eta_{c2}(3^1D_2)$	2	0	2	4.4718	4.4718	—	—
	$\psi(3^3D_1)$	2	1	1	4.4492	4.4492	—	—
	$\psi_2(3^3D_2)$	2	1	2	4.4704	4.4719	—	—
	$\psi_3(3^3D_3)$	2	1	3	4.4816	4.4810	—	—

Table 1: Continued.

n	Meson	L	S	J	Our calculated mass using an artificial neural network (GeV)	Theoretical mass [53] using the shooting method (GeV)	Theoretical mass [54] with NR potential model (GeV)	Exp. mass (GeV) [55]
4D	$\eta_{c2}(4^1D_2)$	2	0	2	4.7562	4.7574	—	—
	$\psi(4^3D_1)$	2	1	1	4.73388	4.7339	—	—
	$\psi_2(4^3D_2)$	2	1	2	4.7573	4.7573	—	—
	$\psi_3(4^3D_3)$	2	1	3	4.7675	4.7675	—	—
1F	$h_{c3}(1^1F_3)$	3	0	3	4.0252	4.0256	4.026	—
	$\chi_2(1^3F_2)$	3	1	2	4.283	4.0283	4.029	—
	$\chi_3(1^3F_3)$	3	1	3	4.02871	4.0287	4.029	—
	$\chi_4(1^3F_4)$	3	1	4	4.0216	4.0212	4.021	—
2F	$h_{c3}(2^1F_3)$	3	0	3	4.34993	4.3499	4.350	—
	$\chi_2(2^3F_2)$	3	1	2	4.34631	4.3494	4.351	—
	$\chi_3(2^3F_3)$	3	1	3	4.3522	4.3522	4.352	—
	$\chi_4(2^3F_4)$	3	1	4	4.3449	4.3476	4.348	—
3F	$h_{c3}(3^1F_3)$	3	0	3	4.64292	4.6429	—	—
	$\chi_2(3^3F_2)$	3	1	2	4.64031	4.6403	—	—
	$\chi_3(3^3F_3)$	3	1	3	4.64493	4.6448	—	—
	$\chi_4(3^3F_4)$	3	1	4	4.6422	4.6422	—	—
4F	$h_{c3}(4^1F_3)$	3	0	3	4.91371	4.9137	—	—
	$\chi_2(4^3F_2)$	3	1	2	4.90957	4.9095	—	—
	$\chi_3(4^3F_3)$	3	1	3	4.91535	4.9153	—	—
	$\chi_4(4^3F_4)$	3	1	4	4.91409	4.9141	—	—

The derivatives of θ_k concerning network parameters, weights, and thresholds can be calculated as follows:

$$\begin{aligned}
\frac{\partial O_k}{\partial w_{ij}} &= w_{jk}\sigma^1(n_j)n_i,\\
\frac{\partial O_k}{\partial w_{jk}} &= \sigma(n_j)\delta_{kk'},\\
\frac{\partial O_k}{\partial w_{ij}} &= w_{jk}\sigma^1(n_j),\\
\frac{\partial O_k}{\partial w_{jk}} &= \delta_{kk'}.
\end{aligned} \tag{4}$$

We followed the formalism used by Lagaris et al. [30] and Mutuk [16–20] for the implementation of ANN to solve the Schrodinger wave equation for the charmonium system. First, we provide the steps for solving any differential equation by employing ANNs under this technique [16–20, 30]. Consider the following differential equation involving a linear operator H, a known function $f(r)$, and $\Psi(r)$ being 0 at boundaries:

$$H\Psi(r) = f(r). \tag{5}$$

Take a trial wave function$\Psi_t(r)$to represent$\Psi(r)$such that

$$\Psi_t(r) = A(r) + B(r,\lambda)N(r,p), \tag{6}$$

where the functions $A(r)$ and $B(r,\lambda)$ are defined in such a way that $\Psi_t(r)$ satisfies the boundary conditions regardless of p (weights and biases of neural networks) and λ values, with $N(r,p)$ being the ANN output function. The collocation method [16–20, 30] is used to convert the above differential equation into a minimization problem.

$$\min_{p,\lambda}\sum_i [H\Psi_t(r_i) - f(r_i)]^2. \tag{7}$$

For the Schrödinger wave equation, the above differential equation takes the following form:

$$H\Psi(r) = \varepsilon\Psi(r). \tag{8}$$

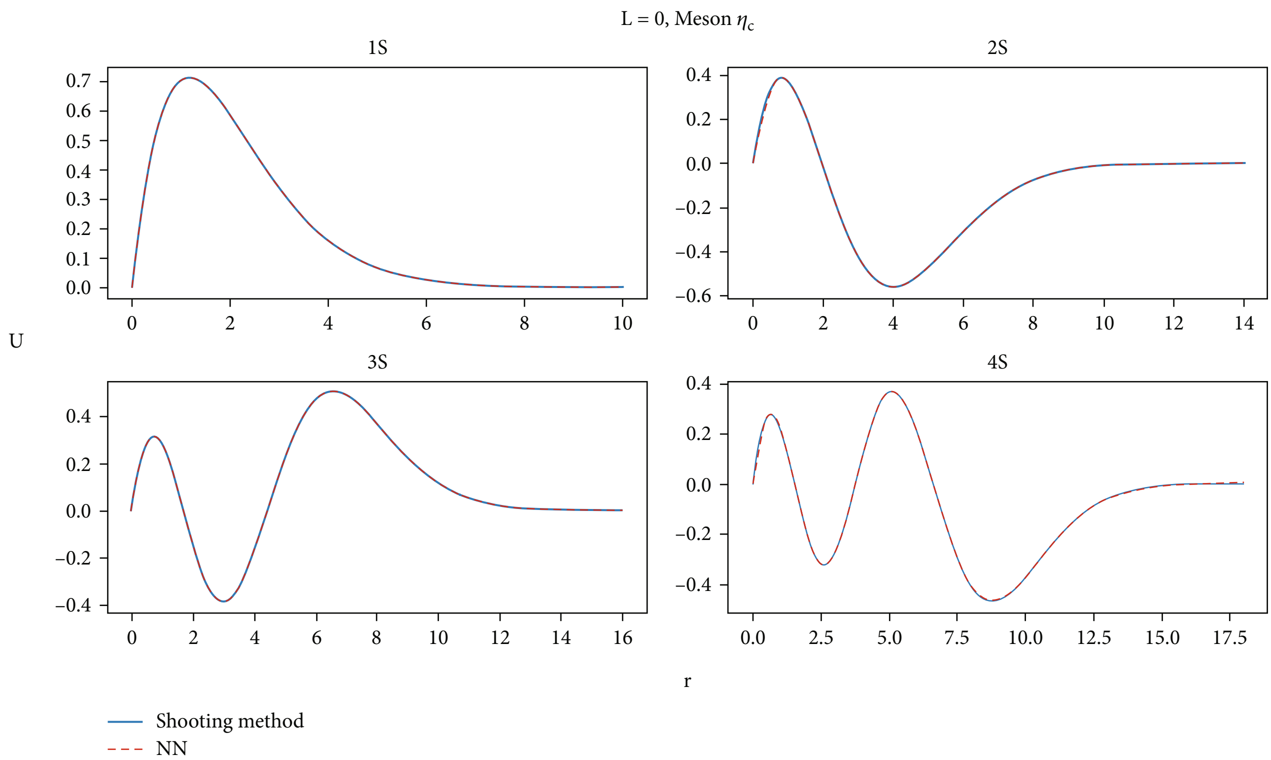

FIGURE 3: Comparison of the wave functions for ground and excited states of η_c are reported using neural networks and shooting methods.

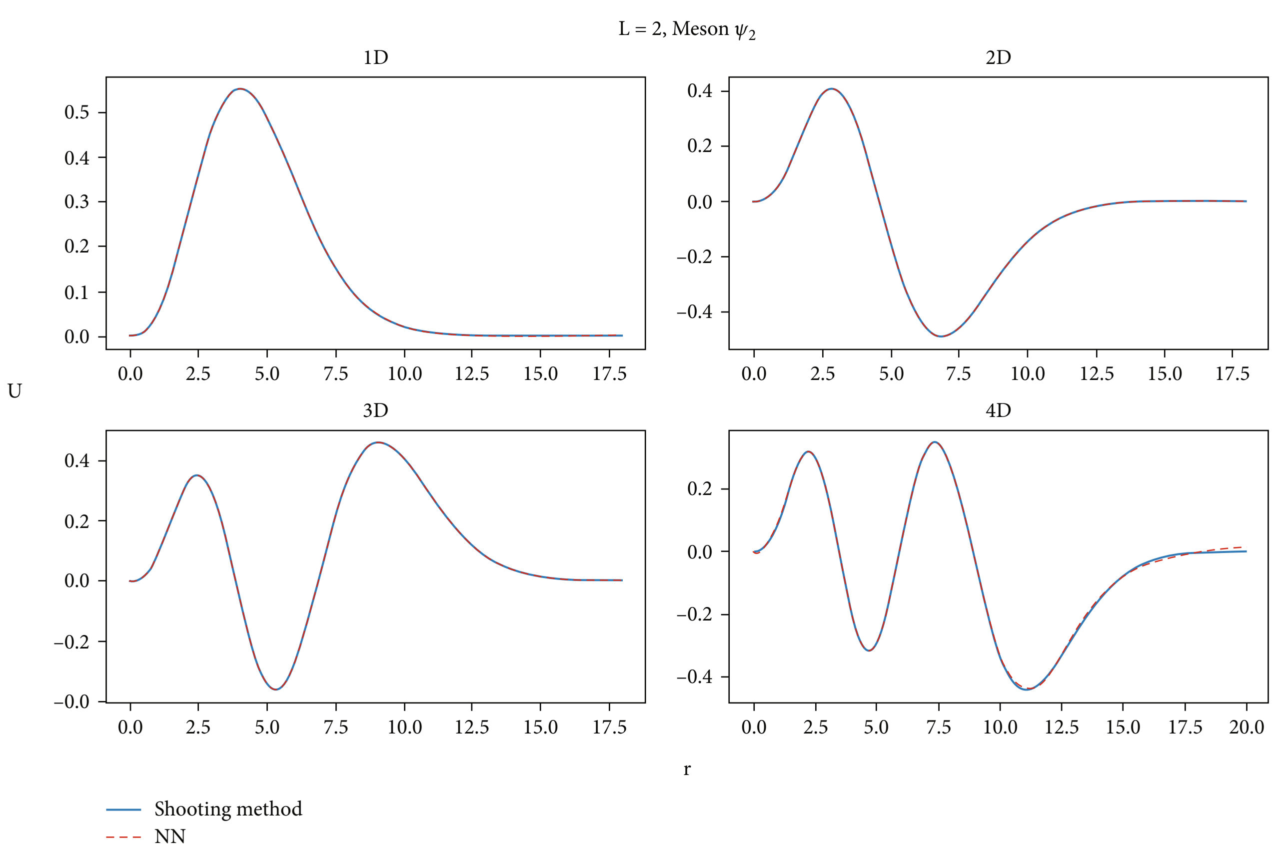

FIGURE 4: Comparison of the wave functions for ground and excited states of ψ_2 are reported using neural networks and shooting methods.

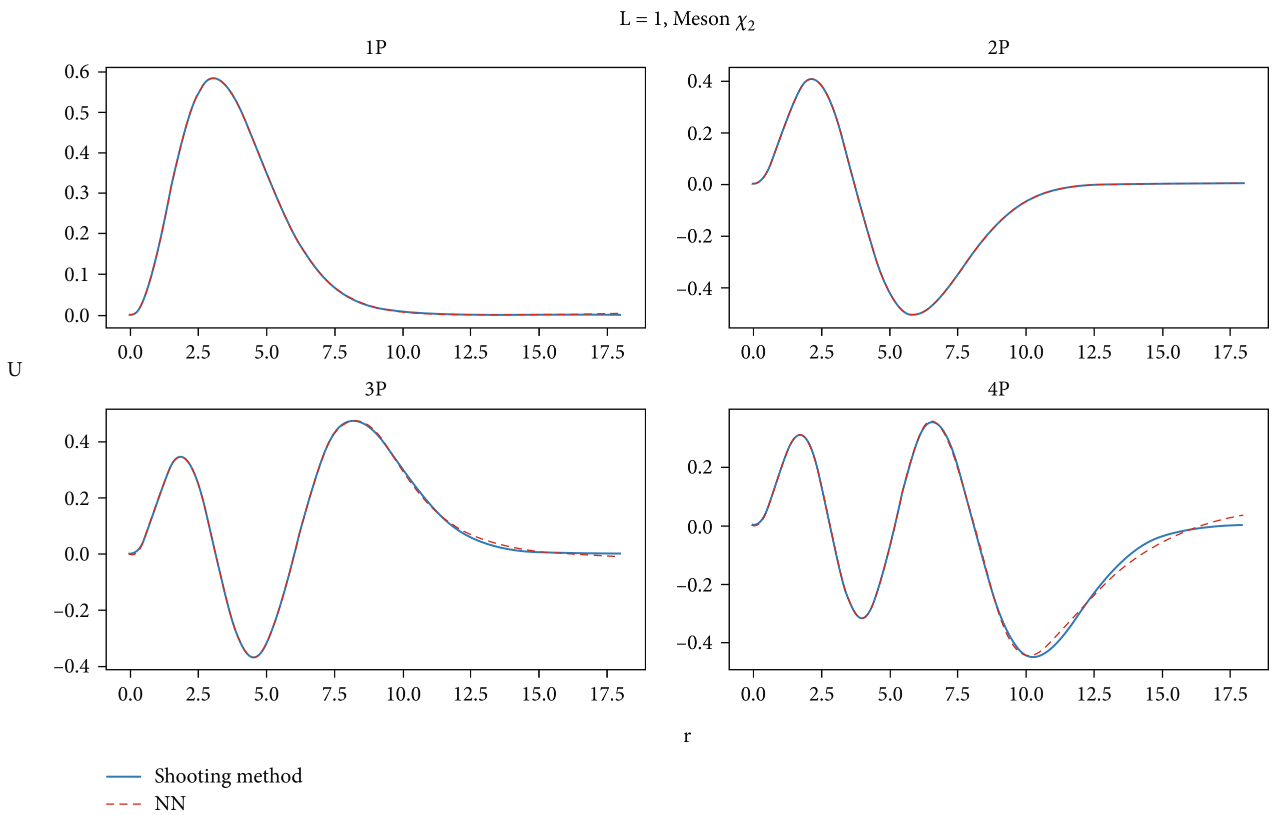

Figure 5: Comparison of the wave functions for ground and excited states of χ_2 are reported using neural networks and shooting methods.

The trial solution can be written as

$$\Psi_t(r) = B(r, \lambda) N(r, p), \quad (9)$$

where $B(r, \lambda) = 0$ at boundaries for a range of λ. This problem can be transformed into a discretization problem by discretizing the domain concerning p and λ. The corresponding error function E is defined as

$$E(p, \lambda) = \frac{\sum_i [H\Psi_t(r_i, p, \lambda) - \varepsilon \Psi_t(r_i, p, \lambda)]^2}{\int |\Psi_t|^2 dr}, \quad (10)$$

where ε can be computed as

$$\varepsilon = \frac{\int \Psi_t{}^* H \Psi_t dr}{\int |\Psi_t|^2 dr}. \quad (11)$$

Let us consider the neural network with n input neurons, m neurons in the hidden layer, and one neuron in the output layer. The output of the network with the input vector $\boldsymbol{r} = (r_1, r_2, \cdots \cdots \cdots, r_n)$ is computed as

$$N = \sum_{i=1}^{m} v_i \sigma(z_i), \quad (12)$$

where $\sigma(z)$ is the sigmoid function and z is defined as

$$z_i = \sum_{j=1}^{n} w_{ij} r_j + b_i. \quad (13)$$

The derivatives of the network output can be defined as

$$\frac{\partial^k N}{\partial r_j^k} = \sum_{i=1}^{m} v_i w_{ij}^k \sigma_i^{(k)}, \quad (14)$$

where $\sigma_i = \sigma(z_i)$ and $\sigma^{(k)}$ is the kth-order derivative of the sigmoid. Once the derivatives of the error concerning network parameters have been defined, any minimization technique can be carried out. By employing this approach, we obtained the neural network output function $N(r, p)$ used for getting the eigen solutions of the Schrodinger equation under the conditions described above and thus obtained the associated energy eigenvalues ε as well. The obtained results are provided in the following section.

4. Results and Discussion

In the field of Hadron physics, the study of radial excitations of mesons is of great interest. Specific potential models serve as a description of the physical environment of mesons and

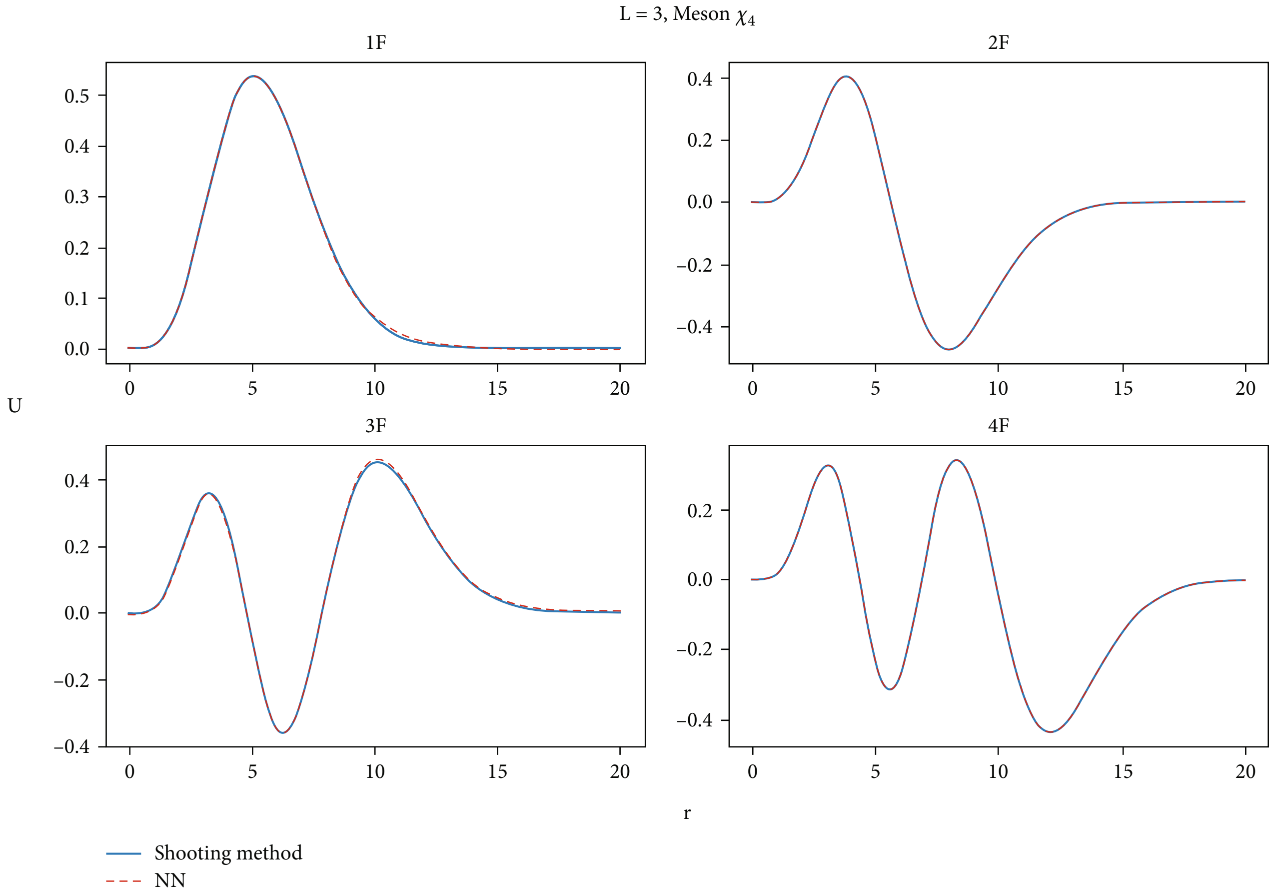

FIGURE 6: Comparison of the wave functions for ground and excited states of χ_4 are reported using neural networks and shooting methods.

serve as a basis for theoretical predictions regarding the characteristics of the charmonium spectrum. The main objective of our study is to investigate the spectrum of charmonia by using the ANN approach. For this purpose, we have computed solutions of the Schrödinger wave equation with the following quark-antiquark effective potential [50, 51] using an artificial neural network.

$$V_{q\bar{q}}(r) = \frac{-4\alpha_s}{3r} + br + \frac{32\pi\alpha_s}{9m_c^2}\left(\frac{\sigma}{\sqrt{\pi}}\right)^3 e^{-\sigma^2 r^2}\overrightarrow{S_c}\cdot\overrightarrow{S_{\bar{c}}} + \frac{1}{m_c^2}\left[\left(\frac{2\alpha_s}{r^3} - \frac{b}{2r}\right)\vec{L}\cdot\vec{S} + \frac{4\alpha_s}{r^3}T\right], \tag{15}$$

where m_c is the mass of the charm quark, the first term $(-4\alpha_s/3r)$ represents strong potential due to gluon exchange with the quark-gluon coupling constant α_s, the second term (br) is the linear confining potential with string tension b, the third term $((32\pi\alpha_s/9m_c^2)(\sigma/\sqrt{\pi})^3 e^{-\sigma^2 r^2}\overrightarrow{S_c}\cdot\overrightarrow{S_{\bar{c}}})$ is the Gaussian-smeared hyperfine spin-spin interaction potential, and the last term $(1/m_c^2)[((2\alpha_s/r^3) - (b/2r))\vec{L}\cdot\vec{S} + (4\alpha_s/r^3)T]$ is the spin-orbit potential. Different parts of the above potential are described below:

$$\overrightarrow{S_c}\cdot\overrightarrow{S_{\bar{c}}} = \frac{S(S+1)}{2} - \frac{3}{4},$$
$$\vec{L}.\vec{S} = \frac{[J(J+1) - L(L+1) - S(S+1)]}{2},$$
$$<^3L_J|T|^3L_J> = \begin{cases} -\dfrac{1}{6(2L+3)}, J = L+1, \\ +\dfrac{1}{6}, J = L, \\ -\dfrac{L+1}{6(2L-1)}, J = L-1, \end{cases} \tag{16}$$

where L is the relative orbital angular momentum of the quark-antiquark pair and S is the total spin angular momentum of the meson.

In this potential model, the used parameters ($\alpha_s = 0.5461$, $b = 0.1425\,\text{GeV}^2$, $\sigma = 1.0946\,\text{GeV}$, and $m_c = 1.4796\,\text{GeV}$) of charm and anticharm quarks were obtained through fitting the experimentally available masses of charmonia [53, 54]. The following radial Schrödinger equation was used to calculate $U(r) = r\,R(r)$:

$$U''(r) + 2\mu\left(E - V(r) - \frac{L(L+1)}{2\mu r^2}\right)U(r) = 0, \tag{17}$$

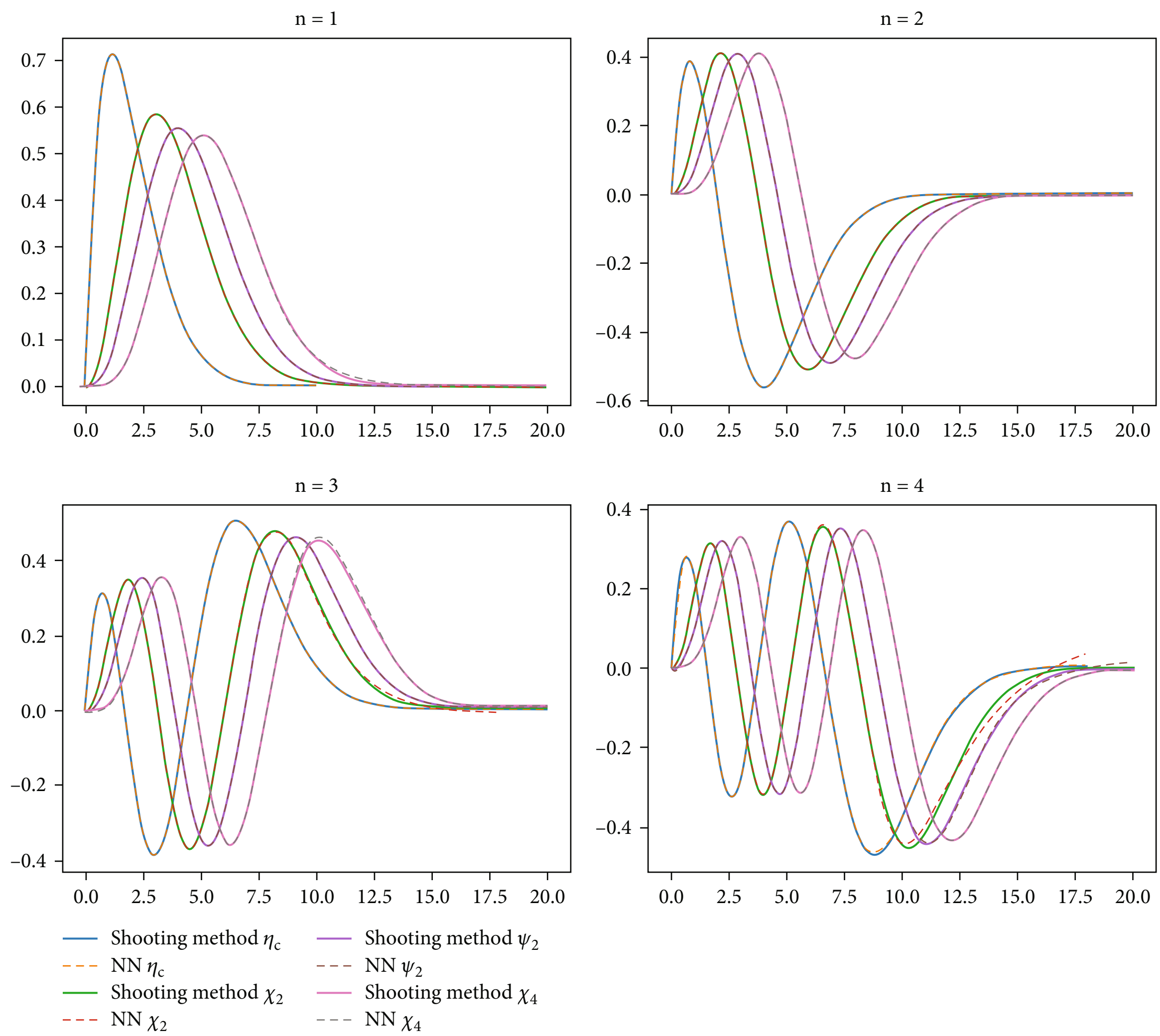

FIGURE 7: Comparison of the wave functions for ground and excited states of η_c, ψ_2, χ_2, and χ_4 are reported using neural networks and shooting methods.

where r is the interquark distance, μ is the reduced mass of quark and antiquark, and $R(r)$ is the radial wave function. The masses of $c\bar{c}$ states are obtained by adding the energy E to the constituent quark masses. For mesons with $L > 0$, results using artificial neural networks are obtained by adding a small enough value in the denominator of the term $1/r^3$ such that it does not affect the results when r approaches zero. In Table 1, we have shown the results of the charmonium mass spectrum obtained through the implementation of our neural network approach. The neural network results are also compared with the already-reported theoretical and experimental results about the charmonium mass spectrum.

Among all the states reported in Table 1, we have plotted the wave functions of ground and radially excited states of η_c, ψ_2, χ_2, and χ_4 for different values of n, S, and L. Each of Figures 3–7 consists of four panels corresponding to $n = 1, 2, 3, \text{and } 4$, respectively, and is compared with the corresponding wave functions produced with the shooting method. The neural results are excellently consistent with the well-established approach of the shooting method, which indicates that the neural network approach works very well. Thus, the graphs express the significance of the method used in providing solutions to the Schrödinger wave equation for the mass spectrum. In all graphs, r is taken along the horizontal axis, and the wave function $U(r)$ is along the vertical axis.

The computed wave functions through the neural network approach can be further used for extracting important information about properties of charmonia, such as the root mean square radii of charmonia, which can be approximated by using the following formula, which employs normalized wave function [53].

$$\sqrt{\langle r^2 \rangle} = \sqrt{\int U^* r^2 \, U \, dr}, \qquad R(0) = U'(0) \text{ for } l = 0. \tag{18}$$

The radial wave function at origin is used for many purposes in high-energy physics; for details, see ref [53].

5. Conclusion

We solved the Schrodinger wave equation for the complete nonrelativistic QCD potential by using the ANN approach. The solutions of the Schrodinger equation were used to predict masses of the ground and radially excited states of charmonia. The ANN results were compared with the numerical and experimental results already reported. The ANN mass spectrum predictions and their associated wave functions are found to be in excellent agreement with their competitive results. This indicates the excellence of the ANN approach in predicting the charmonium mass spectrum. As discussed in the literature survey section, the ANN approach is a more efficient, more general, and continuous solution provider as compared to numerical approaches, which might skip some regions of mass spectroscopy.

Data Availability

Data and code will be made available on a reasonable request.

Conflicts of Interest

There are no conflicting interests, according to the authors.

References

[1] CERN, *CERN Accelerating Science*, CERN, 2019, September 2019, https://home.cern/science/physics/standard-model.

[2] A. Radovic, M. Williams, D. Rousseau et al., "Machine learning at the energy and intensity frontiers of particle physics," *Nature*, vol. 560, no. 7716, pp. 41–48, 2018.

[3] R. Fayyazuddin, *A Modern Introduction to Particle Physics*, World Scientific, 3rd edition, 2012.

[4] F. Mandl and G. Shaw, *Quantum Field Theory*, John Wiley & Sons, 2nd edition, 2010.

[5] W. Roberts and B. Silvestre-Brac, "General method of calculation of any hadronic decay in the $^3P_0$ model," *Few-Body Systems*, vol. 11, no. 4, pp. 171–193, 1992.

[6] M. Pillai, J. Goglio, and T. G. Walker, "Matrix Numerov method for solving Schrödinger's equation," *American Journal of Physics*, vol. 80, no. 11, pp. 1017–1019, 2012.

[7] G. Gulyamov, A. B. Davlatov, S. T. Inoyatov, and S. A. Makhmudov, "Calculation of the energy levels and wave functions of electrons in nanowires by the shooting method," *Journal of Applied Science and Engineering*, vol. 25, no. 1, pp. 31–36, 2022.

[8] J. Kafle, A. Kafle, and C. N. Tiwari, "Numerical solution of Schrödinger equation by using Crank-Nicolson method," *Journal of Nepal Physical Society*, vol. 9, no. 1, pp. 29–37, 2023.

[9] I. Aleksander, "Designing conscious systems," *Cognitive Computation*, vol. 1, pp. 22–28, 2009.

[10] B. J. Baars and S. Franklin, "An architectural model of conscious and unconscious brain functions: global workspace theory and IDA," *Neural Networks*, vol. 20, no. 9, pp. 955–961, 2007.

[11] N. Yadav, A. Yadav, and M. Kumar, *An Introduction to Neural Network Methods for Differential Equations*, Springer Briefs in Applied Sciences and Technology, Springer, 2015.

[12] B. H. Denby, "Neural networks and cellular automata in experimental high energy physics," *Computer Physics Communications*, vol. 49, no. 3, pp. 429–448, 1988.

[13] C. Peterson, T. Rognvaldsson, and L. Lonnblad, "JETNET 3.0–a versatile artificial neural network package," *Computer Physics Communications*, vol. 81, pp. 185–220, 1994.

[14] P. Baldi, K. Cranmer, T. Faucett, P. Sadowski, and D. Whiteson, "Parametrized neural network for high-energy physics," *The European Physical Journal C*, vol. 76, no. 235, 2016.

[15] G. Carleo, I. Cirac, K. Cranmer et al., "Machine learning and the physical sciences," 2019, http://arxiv.org/abs/1903.10563.

[16] H. Mutuk, "A neural network study of Blasius equation," 2018, http://arxiv.org/abs/1811.08936.

[17] H. Mutuk, "Cornell potential: a neural network approach," *Advances in High Energy Physics*, vol. 2019, Article ID 3105373, 9 pages, 2019.

[18] H. Mutuk, "Energy levels of one-dimensional anharmonic oscillator via neural networks," *Modern Physics Letters A*, vol. 34, no. 12, article 1950088, 2019.

[19] H. Mutuk, "Mass spectrum of exotic X (5568) state via artificial neural network," 2019, http://arxiv.org/abs/1901.01154.

[20] H. Mutuk, "Neural network study of hidden-charm pentaquark resonances," 2019, http://arxiv.org/abs/1904.09756v3.

[21] DELPHI Collaboration, P. Abreu, W. Adam et al., "Classification of hadronic decays of Z0 into b and c quark pairs using neural network," *Physics Letters B*, vol. 295, no. 3-4, pp. 383–395, 1992.

[22] H. Kolanoski, "Application of artificial neural networks in particle physics," in *Artificial Neural Networks — ICANN 96. ICANN 1996*, C. Malsburg, W. Seelen, J. C. Vorbrüggen, and B. Sendhoff, Eds., vol. 1112 of Lecture Notes in Computer Science, Springer, Berlin, Heidelberg, 1996.

[23] ATLAS collaboration, J. A. Aguilar-Saavedra, S. P. Amor Dos Santos et al., "A neural network clustering algorithm for the ATLAS silicon pixel detector," *Journal of Instrumentation*, vol. 9, no. 9, 2014.

[24] C. Peterson, "Track finding with neural networks," *Nuclear Instruments and Methods in Physics Research Section A: Accelerators, Spectrometers, Detectors and Associated Equipment*, vol. 279, no. 3, pp. 537–545, 1989.

[25] L. Lonnblad, C. Peterson, and T. Rognvaldsson, "Finding gluon jets with a neural trigger," *Physical Review Letters*, vol. 65, no. 11, pp. 1321–1324, 1990.

[26] H. Bruce, M. Denby, F. B. Campbell, N. Chriss, C. Bowers, and F. Nesti, "Neural networks for triggering," *IEEE Transactions on Nuclear Science*, vol. 37, no. 2, pp. 248–254, 1990.

[27] R. Frhwirth, M. Regler, R. K. Bock, H. Grote, and D. Notz, *Data Analysis Techniques for High Energy Physics*, Cambridge monographs, 1990.

[28] A. Strandlie and R. Frhwirth, "Track and vertex reconstruction: from classical to adaptive methods," *Reviews of Modern Physics*, vol. 82, no. 2, pp. 1419–1458, 2010.

[29] G. Carleo and M. Troyer, "Solving the quantum many-body problem with artificial neural networks," *Science*, vol. 355, no. 6325, pp. 602–606, 2017.

[30] E. I. Lagaris, A. Likas, and D. I. Fotiadis, "Artificial neural networks for solving ordinary and partial differential equations,"

IEEE Transactions on Neural Networks, vol. 9, no. 5, pp. 987–1000, 1998.

[31] D. W. Berry, "High-order quantum algorithm for solving linear differential equations," *Journal of Physics A: Mathematical and Theoretical*, vol. 47, no. 10, article 105301, 2014.

[32] Y. Cao, A. Papageorhiou, I. Petras, J. Traub, and S. Kais, "Quantum algorithm and circuit design solving the Poisson equation," *New Journal of Physics*, vol. 15, no. 1, 2013.

[33] K. K. Sharma, "Quantum machine learning in high energy physics: the future prospects," *High Energy Particle Physics*, vol. 6, 2018.

[34] S. Carrazza, "Machine learning challenges in theoretical HEP," 2017, http://arxiv.org/abs/1711.10840.

[35] A. J. da Silva, T. B. Ludermir, and W. R. de Oliveira, "Quantum perceptron over a field and neural network architecture selection in a quantum computer," *Neural Networks*, vol. 76, pp. 55–64, 2016.

[36] F. Tacchino, C. Macchiavello, D. Gerace, and D. Bajon, "An artificial neuron implemented on an actual quantum processor," *npj Quantum Information*, vol. 5, no. 26, 2019.

[37] E. I. Lagaris, A. Likas, and D. I. Fotiadis, "Artificial neural network methods in quantum mechanics," *Computer Physics Communications*, vol. 104, no. 1-3, pp. 1–14, 1997.

[38] M. J. Sugawara, "Numerical solution of the Schrödinger equation by neural network and genetic algorithm," *Computer Physics Communications*, vol. 140, no. 3, pp. 366–380, 2001.

[39] O. D. Damazio and M. J. de Seixas, "Neural networks to identify particles using topological properties of the calorimeter," *Sba: Controle & Automação Sociedade Brasileira de Automatica*, vol. 15, pp. 62–70, 2004.

[40] L. Teodorescu, "Artificial neural network in high-energy physics," 2008, https://cds.cern.ch/record/1100521.

[41] "CDF experiment," http://www-cdf.fnal.gov.

[42] "BaBar experiment," http://www.slac.stanford.edu/BFROOT/.

[43] "DZero experiment," http://www-d0.fnal.gov.

[44] L. W. Miranker, "A neural network wave formalism," *Advances in Applied Mathematics*, vol. 37, no. 1, pp. 19–30, 2006.

[45] J. Therhaag, "Introduction to neural networks in high energy physics," *EPJ Web of Conferences*, vol. 55, article 02003, 2013.

[46] A. Radi and S. K. Hindawi, "Applying artificial neural network hadron-hadron collisions at LHC," in *Artificial Neural Networks: Architectures and Applications*, S. Kenji, Ed., pp. 183–201, BoD-Books on Demand, 2013.

[47] P. Sadowski, P. Baldi, and D. Whiteson, "Searching for Higgs boson decay modes with deep learning," in *NIPS'14: Proceedings of the 27th International Conference on Neural Information Processing Systems-Volume 2*, pp. 2393–2401, MIT Press, 2014.

[48] J. Hermann, Z. Schätzle, and F. Noé, "Deep neural network solution of the electronic Schrödinger equation," 2020, http://arxiv.org/abs/1909.08423v5.

[49] H. Mutuk, "Energy Levels of the one-dimensional anharmonic oscillator via neural network," 2018, http://arxiv.org/abs/1811.08893v1.

[50] K. K. Sharma, "Quantum machine learning and its supremacy in high energy physics," 2020, http://arxiv.org/abs/2011.11478v1.

[51] S. Manzhos, "Machine learning for the solution of the Schrödinger equation," *Machine Learning: Science and Technology*, vol. 1, no. 1, article 013002, 2020.

[52] C. Lema and A. Choromanska, "Approximating ground state energies and wave functions of physical systems with neural networks," 2020, https://arxiv.org/abs/2011.10694.

[53] A. Sultan, N. Akbar, B. Masud, and F. Akram, "Higher hybrid charmonia in an extended potential model," *Physical Review D*, vol. 90, no. 5, article 054001, 2014.

[54] T. Barnes, S. Godfrey, and E. S. Swanson, "Higher charmonia," *Physical Review D*, vol. 72, no. 5, article 054026, 2005.

[55] J. Beringer, J. F. Arguin, R. M. Barnett et al., "Review of Particle physics," *Physical Review D*, vol. 86, no. 1, article 010001, 2012.